



## Microstructure and room temperature mechanical properties of directionally solidified Mg–2.35Gd magnesium alloy

Jia-he WANG<sup>1,2</sup>, Guang-yu YANG<sup>1,2</sup>, Shao-jun LIU<sup>1,2</sup>, Wan-qi JIE<sup>1,2</sup>

1. School of Materials Science and Engineering, Northwestern Polytechnical University, Xi'an 710072, China;
2. State Key Laboratory of Solidification Processing, Northwestern Polytechnical University, Xi'an, 710072, China

Received 14 June 2015; accepted 24 February 2016

**Abstract:** Directional solidification of Mg–2.35Gd (mass fraction, %) magnesium alloy was carried out to investigate the effects of the solidification parameters (growth rate  $v$  and temperature gradient  $G$ ) on microstructure and room temperature mechanical properties under the controlled solidification conditions. The specimens were solidified under steady state conditions with different temperature gradients ( $G=20, 25$  and  $30$  K/mm) in a wide range of growth rates ( $v=10\text{--}200$   $\mu\text{m/s}$ ) by using a Bridgman-type directional solidification furnace with liquid metal cooling (LMC) technology. The cellular microstructures are observed. The cellular spacing  $\lambda$  decreases with increasing  $v$  for constant  $G$  or with increasing  $G$  for constant  $v$ . By using a linear regression analysis the relationships can be expressed as  $\lambda=136.216v^{-0.2440}$  ( $G=30$  K/mm) and  $\lambda=626.5630G^{-0.5625}$  ( $v=10$   $\mu\text{m/s}$ ), which are in a good agreement with Trivedi model. An improved tensile strength and a corresponding decreased elongation are achieved in the directionally solidified experimental alloy with increasing growth rate and temperature gradient. Furthermore, the directionally solidified experimental alloy exhibits higher room temperature tensile strength than the non-directionally solidified alloy.

**Key words:** Mg–2.35Gd alloy; directional solidification; cellular spacing; microstructure; mechanical property

### 1 Introduction

In directional solidification, the solidification parameters such as temperature gradient ( $G$ ) and solidification rate ( $v$ ) can be independently controlled, which make it possible to study effects of  $G$  and  $v$  on the microstructure of an alloy. Directional solidification technology has been widely used in some kinds of alloys such as aluminum alloys and superalloys, but there are only limited investigations on magnesium alloys [1,2]. ZHANG et al [3] and ZHENG et al [4] studied the morphologies and microsegregation of directionally solidified Mg–4Al alloy and AX44 (Mg–4Al–4Ca, mass fraction, %) alloy using electron probe microanalysis (EPMA) and the Scheil-solidification model. PETERSEN et al [5] studied dendrite crystallography of directionally solidified AZ91 magnesium alloy. MIRKOVIC et al [6] analyzed the microsegregation of directionally solidified AZ31 and AM50 castings. However, these previous researches are mainly focused on Mg–Al-based alloys and few works are reported on

Mg–RE-based alloys.

Mg–RE (rare-earth elements, such as Gd, Y, Nd misch metal)-based alloys have received tremendous attention due to their high specific strength both at room and elevated temperatures as well as their excellent creep resistance [7,8]. Among them, Mg–Gd-based alloy is one of the promising candidates for a novel Mg-based heat-resistant alloy. There have been extensive researches on microstructures and the mechanical properties of Mg–Gd-based alloys [9–11]. NISHIJIMA and HIRAGA [9] studied structural changes of the precipitates in Mg–5%Gd (mole fraction) alloy by aging at 200 and 250 °C. HONMA et al [10] investigated the microstructures of age hardened Mg–2.0Gd–1.2Y– $x$ Zn–0.2Zr ( $x=0, 0.3\%$  and  $1.0\%$ , mole fraction) alloys to understand the remarkable age-hardening and unusual plastic elongation behavior. NIE et al [11] studied the solute segregation and the precipitate phases in creep-resistant Mg–1Gd–0.4Zn–0.2Zr (mole fraction, %) alloy isothermally aged at 250 and 200 °C using the three-dimensional atom probe and high-angle annular dark-field scanning transmission electron microscopy (TEM). However,

there are few works reported on the solidification behaviors of Mg–Gd binary alloys under different casting conditions, in particular, under directional solidification condition.

The objective of the present study is to investigate influences of  $G$  and  $v$  on the microstructures of Mg–2.35Gd magnesium alloy and to establish the quantitative relationship between characteristic length scales and growth processing parameters under the controlled directional solidification conditions. The obtained results enable us to predict and control directionally solidified microstructures and mechanical properties of the tested alloy system.

## 2 Experimental

### 2.1 Alloy preparation

Mg–2.35Gd alloys were prepared from pure Mg (99.98%) and Mg–28Gd (mass fraction, %) master alloy by melting in an electrical resistance furnace under the protection of anti-oxidizing flux (RJ–4). After refining with  $C_2Cl_6$  and holding at 780 °C for 20 min, the melts were poured into an iron test bar mold ( $d10\text{ mm} \times 150\text{ mm}$ ) at 740 °C. The test bars were further processed into the samples of  $d\ 7.8\text{ mm} \times 90\text{ mm}$  for subsequent directional solidification experiments.

### 2.2 Directional solidification experiments

A high temperature gradient Bridgman-type directional solidification furnace with a graphite heater and a quenching system of water-cooled Ga–In–Sn liquid metals was used. The prepared sample ( $d\ 7.8\text{ mm} \times 90\text{ mm}$ ) was loaded in a special stainless tube crucible with 10 mm in outer diameter (OD), 8 mm in inner diameter (ID), 120 mm in length and sealed ends. A special sulfur dioxide ( $SO_2$ ) generator was inserted into the top of the crucible, which was designed to prevent the oxidation of the experimental alloy [12]. The crucible was put in the vacuum furnace with the graphite heater, pumped down to 1 Pa, backfilled with high-purity Ar, and then heated to 800 °C holding for 30 min. When the required axial temperature gradient was reached, the sample was directionally solidified by moving the crucible downward at a given speed (10–200  $\mu\text{m/s}$ ) for about 40 mm, and subsequently quenched in Ga–In–Sn liquid metals. For the analysis, the withdrawal rate was approximately used as the growth rate.

### 2.3 Sample characterization

For subsequent characterization, the solidified samples were cut along both the longitudinal and transverse sections to investigate the quenched interface morphology and the solidification microstructure. Olympus PM-G3 type optical microscope (OM) was

used to examine the solidification microstructure. The room temperature tensile properties were tested in a Zwick 150 type universal tensile testing machine at a maximum load of 150 kN and a strain rate of 1 mm/min. The test specimens were in rectangular shape with 20 mm in length, 5 mm in width and 2 mm in height, as shown in Fig. 1.

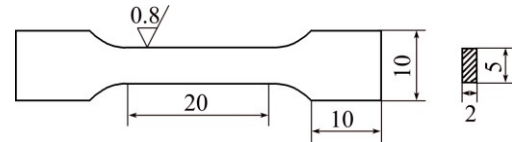


Fig. 1 Specimen dimensions for tensile tests used in this work (unit: mm)

## 3 Results and discussion

### 3.1 Directional solidification microstructures

Figure 2 shows OM images of longitudinal and transversal sections of directionally solidified Mg–2.35Gd alloy at the constant temperature gradient of 30 K/mm and different growth rates. As shown in Figs. 2(a), (c) and (e), the solid/liquid interface of Mg–2.35Gd alloy is a typical cellular interface and the microstructures exhibit typical cellular structures with coarse trunks. Meanwhile, the cellular spacing decreases with increasing growth rate. In the whole growth rate range of 10–200  $\mu\text{m/s}$ , no dendritic structures were observed. In order to further confirm the microstructures, OM images of transversal section of directionally solidified Mg–2.35Gd alloy are shown in Figs. 2(b), (d) and (f). Clearly, the microstructures exhibit typical cellular structure and the shape of the cellular crystals changes from the hexagonal to the square and the circular with increasing growth rate.

According to the dendrite growth theory of KURZ–FISHER [13], the approximate criterion growth rate for cell/dendrite transition ( $v_{c-d}$ ) can be expressed as follows:

$$v_{c-d} = \frac{GD}{\Delta T_0 k} = \frac{GD}{mC_0(k-1)} \quad (1)$$

where  $G$  is the temperature gradient in the liquid,  $D$  is the diffusion coefficient of solute atom in the liquid,  $\Delta T_0$  is the temperature interval between the liquidus and the solidus,  $k$  is the distribution coefficient,  $m$  is the slope of the liquidus and  $C_0$  is the initial content of the solidifying alloy. Using the thermophysical parameters given in Table 1, the  $v_{c-d}$  of Mg–2.35Gd alloy can be evaluated to be 23.4  $\mu\text{m/s}$ .

Obviously, the experimental solidification microstructure is still cellular structure near the theoretical criterion growth rate for cell/dendrite transition, which

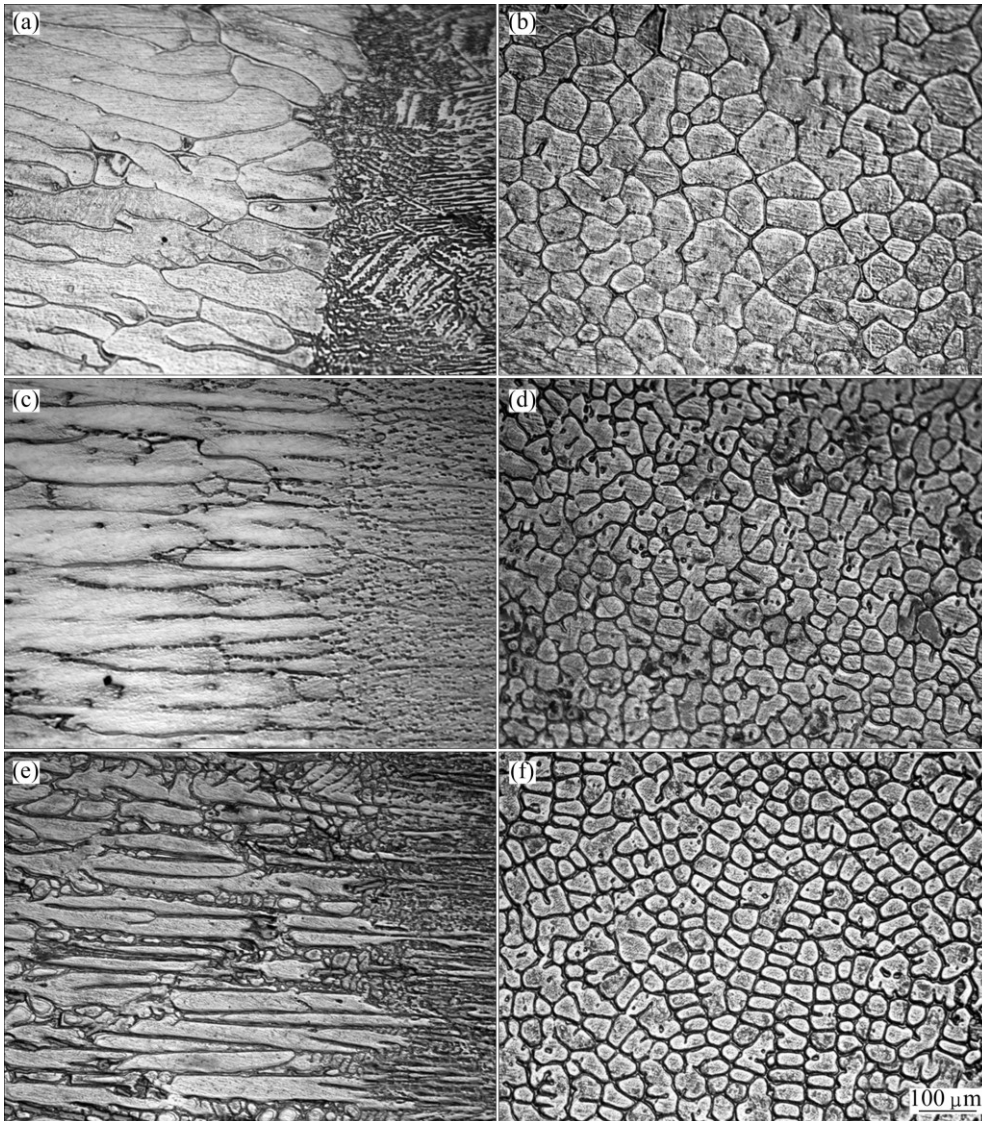


**Fig. 2** OM images of directionally solidified Mg–2.35Gd alloy at  $G=30$  K/mm and growth rates of  $10 \mu\text{m/s}$  (a, b),  $100 \mu\text{m/s}$  (c, d) and  $200 \mu\text{m/s}$  (e, f): (a, c, e) Longitudinal section; (b, d, f) Transverse section

**Table 1** Thermophysical parameters of Mg–2.35Gd alloy

Parameter	Value	Ref.
Initial content, $C_0/\%$	2.35	
Slope of liquid line, $m/(\text{K}\cdot\%^{-1})$	-1.380	
Distribution coefficient, $k$	0.1049	
Diffusion coefficient (liquid), $D/(\text{cm}^2\cdot\text{s}^{-1})$	$1.233\times 10^{-9}$	[14]
Gibbs–Thomson coefficient, $\Gamma/(\text{m}\cdot\text{K})$	$1.1\times 10^{-7}$	[14]

cannot be used to interpret the absence of dendrite structure with increasing or decreasing the growth rate. However, according to the microstructure/processing map proposed by LU and HUNT [15,16] in dimensionless temperature gradient  $G'$  ( $G'=G\Gamma k/\Delta T_0^2$ ) and dimensionless growth rate  $v'$  ( $v'=v\Gamma k/(\Delta T_0^2)$ ),  $\Delta T_0=mC_0(k-1)/k$ ) domains for Al–Cu alloy considering the interfacial energy, as shown in Fig. 3, it is very clear that the solute content has a significant effect on the

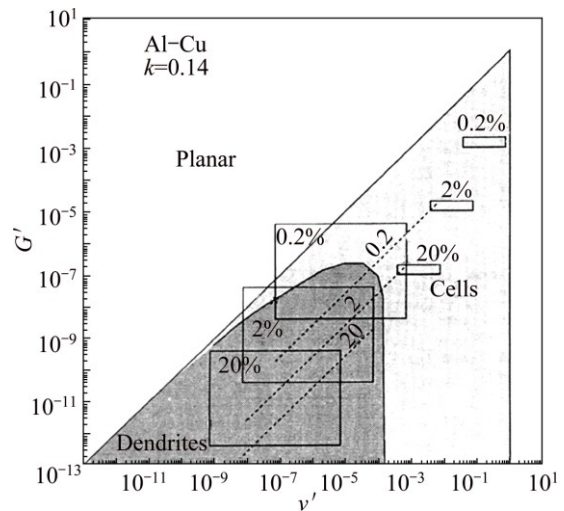


**Fig. 3** Microstructure/processing map in dimensionless  $G'$ – $v'$  domain for Al–Cu alloy [15] (triangular-shaped region indicates that cells and dendrites may form)



morphology evolution. A lower solute content results in a smaller corresponding scope of dendrite and an easier way to obtain high speed cellular structure. In the present investigation, the low Gd concentration in experimental Mg–2.35Gd alloy indicates that only cellular structures may form independent of solidification parameters (dimensionless temperature gradient  $G'$  and growth rate  $v'$ ).

Figure 4 shows OM images of longitudinal and transversal sections of directionally solidified Mg–2.35Gd alloy under different temperature gradients (20, 25 and 30 K/mm) at a constant growth rate of 10  $\mu\text{m/s}$ . The microstructures still exhibit typical cellular structures, and the cellular spacing decreases with increasing temperature gradient.

### 3.2 Directional solidification microstructures parameters

It is well known that the cellular spacing has a

significant effect on the mechanical properties such as yield strength and creep resistance of the alloy. Different theoretical models have been proposed by HUNT and LU [17], KURZ and FISHER [13] and TRIVEDI [18] to characterize the cellular spacing under various solidification conditions, which are given by Eqs. (2)–(4), respectively:

$$\lambda = 2.83[m(k-1)D\Gamma]^{0.25} C_0^{0.25} v^{-0.25} G^{-0.5} \quad (\text{Hunt model}) \quad (2)$$

$$\lambda = 4.3[m(k-1)D\Gamma/k^2]^{0.25} C_0^{0.25} v^{-0.25} G^{-0.5} \quad (\text{Kurz-Fisher model}) \quad (3)$$

$$\lambda = 2.83[m(k-1)D\Gamma L]^{0.25} C_0^{0.25} v^{-0.25} G^{-0.5} \quad (\text{Trivedi model}) \quad (4)$$

where  $\Gamma$  is the Gibbs–Thomson coefficient,  $L$  is a constant with the value of 28 that depends on harmonic perturbations. The thermophysical parameters of experimental Mg–2.35Gd alloy used in the calculations of the above theoretical models are given in Table 1.

Figure 5(a) shows the measured cellular spacing of

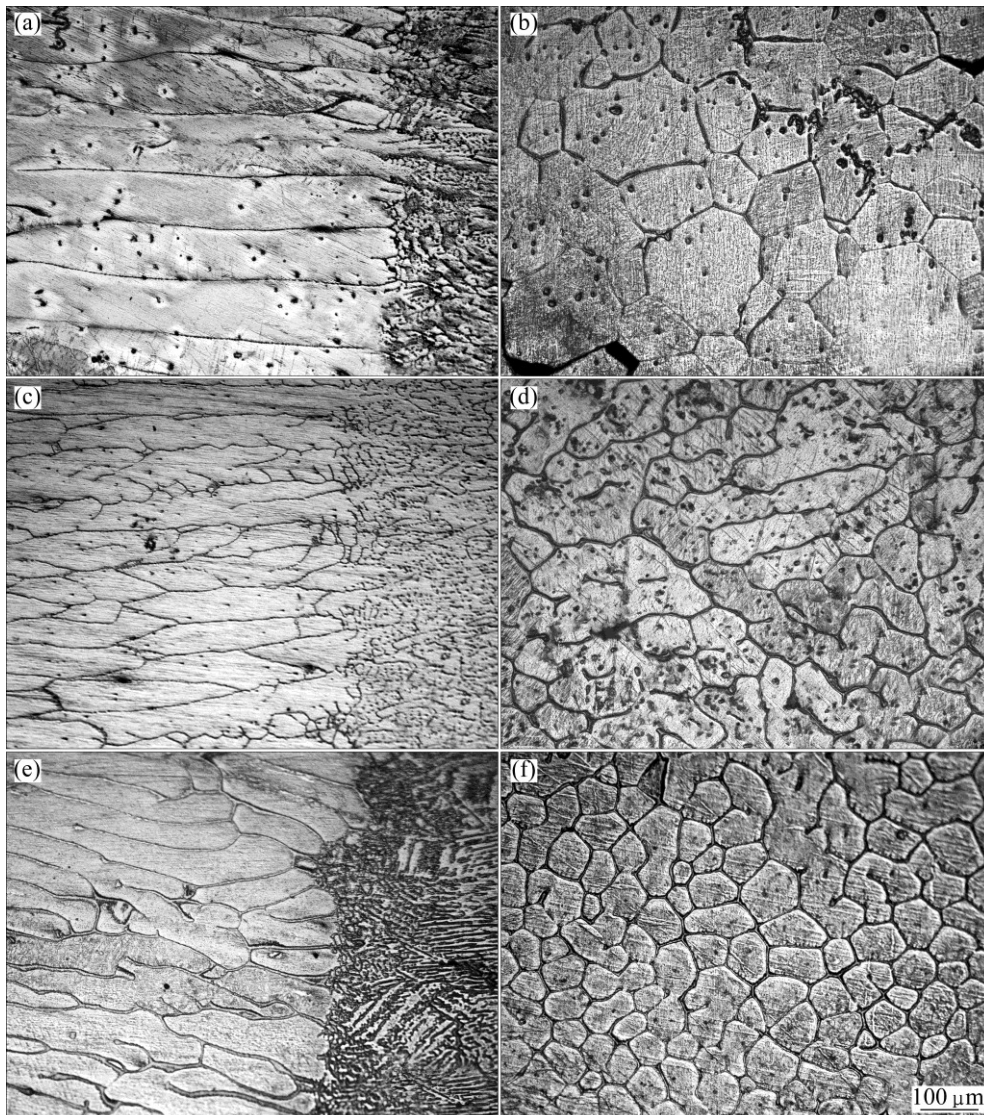


**Fig. 4** OM images of directionally solidified Mg–2.35Gd alloy at  $v=10 \mu\text{m/s}$  and temperature gradients of 20 K/mm (a, b), 25 K/mm (c, d) and 30 K/mm (e, f): (a, c, e) Longitudinal section; (b, d, f) Transverse section

the experimental Mg–2.35Gd alloy with a function of growth rate. Through a linear regression analysis, the relationship between  $\lambda$  and  $v$  at a temperature gradient of 40 K/mm was established as follows:

$$\lambda = 136.216v^{-0.2440} \quad (5)$$

For comparison, the values of cellular spacing calculated by Hunt model, Kurz–Fisher (K–F) model, and Trivedi model are also given in Fig. 5(a). It should be noted that the values calculated by Kurz–Fisher model and Hunt model significantly diverge from the measured results, while the measured results are in a good agreement with the values calculated by Trivedi model. Figure 5(b) shows the measured cellular spacing of the experimental Mg–2.35Gd alloy with a function of temperature gradient. Through a linear regression analysis, the relationship between  $\lambda$  and  $G$  at a growth rate of 10  $\mu\text{m/s}$  was established as follows:

$$\lambda = 626.5630G^{-0.5625} \quad (6)$$

Similar to Fig. 5(a), the values calculated by Hunt model, Kurz–Fisher model and Trivedi model are also

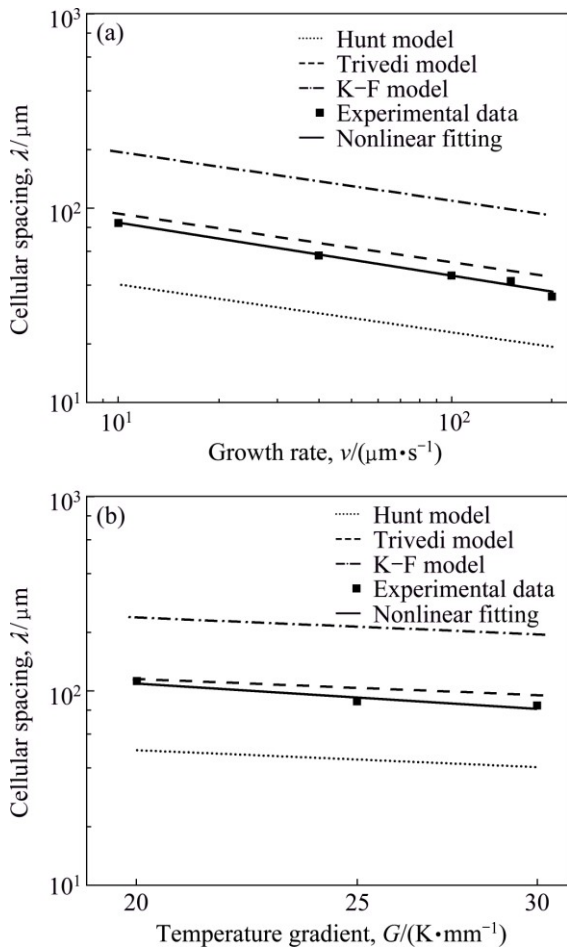


**Fig. 5** Comparison of measured cellular spacing with calculated one by different theoretical models for directionally solidified Mg–2.35Gd alloy: (a) At  $G=30$  K/mm and different growth rates; (b) At  $v=10$   $\mu\text{m/s}$  and different temperature gradients

shown for comparison. Again, the values calculated by Trivedi model are in a good agreement with the measured results. However, the values calculated by Kurz–Fisher model and Hunt model obviously diverge from the measured ones.

Figure 6 shows the comparison of the cellular spacing obtained from the experiments and prediction of theoretical models for Mg–2.35Gd alloy at different growth rates and different temperature gradients. It can be seen that the measured cellular spacing is in good agreement with the theoretical prediction by Trivedi model, indicating that the Trivedi model can be used to predict the cellular spacing of directionally solidified Mg–2.35Gd alloy with a reasonable accuracy.

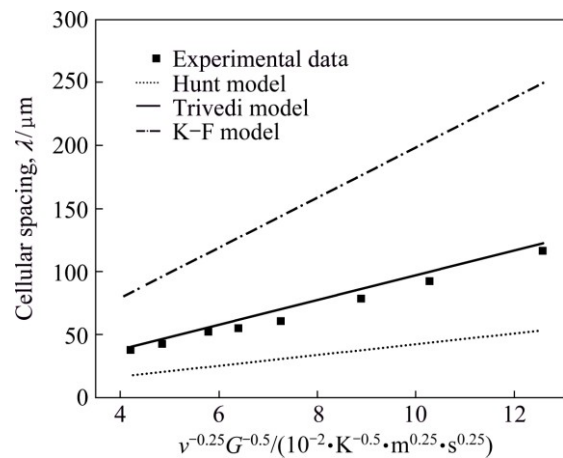


**Fig. 6** Comparison of observed cellular spacing with calculated one by different theoretical models for directionally solidified Mg–2.35Gd alloy at different  $G$  and  $v$  values

### 3.3 Room temperature mechanical properties

Figure 7 shows the nominal stress–nominal strain curves of the directionally solidified and non-directionally solidified experimental alloy at the same cooling rate. The cooling rate of Mg–2.35Gd alloy cast

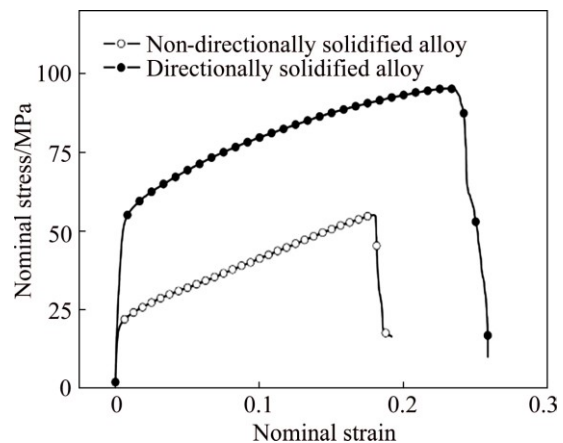


**Fig. 7** Nominal stress–nominal strain curves for directionally solidified and non-directionally solidified Mg–2.35Gd alloys at cooling rate of 2 K/s

by metal mold was measured to be 2 K/s, which was close to that of the directionally solidified experimental alloy at  $G=20$  K/mm and  $v=100$   $\mu\text{m/s}$ . It can be seen that the directional solidification technology can significantly improve the room temperature mechanical properties of the experimental alloy. The ultimate tensile strength (UTS) and elongation to failure are respectively improved from 55 MPa and 14% for the non-directionally solidified alloy to 94 MPa and 18% for the directionally solidified alloy. The directionally solidified alloy exhibits 1.71 times higher in ultimate tensile strength (UTS) and 1.29 times higher in elongation than the non-directionally solidified alloy, which can be due to the fact that directional solidification technology could control the grain orientation, eliminate transverse grain boundary, achieve a sequence solidification in the whole casting process, thereby decreasing the amount of solidification defects, such as shrinkage porosity and shrinkage cavity.

Figure 8 shows the room temperature mechanical properties of Mg–2.35Gd alloy prepared by directional solidification at different  $v$  values for constant  $G$  and different  $G$  values for constant  $v$ , respectively. At

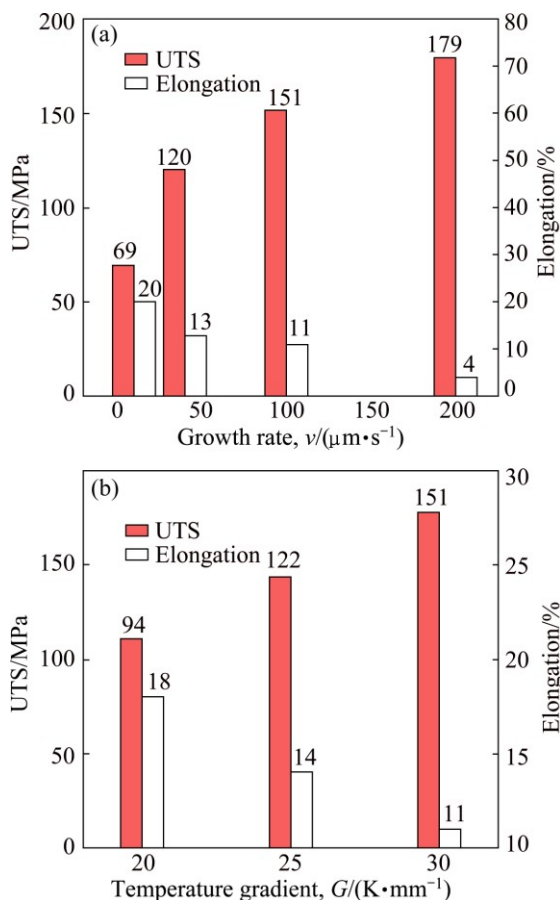


**Fig. 8** Room temperature mechanical properties of directionally solidified Mg–2.35Gd alloy under different conditions: (a) At  $G=30$  K/mm and different growth rates; (b) At  $v=100$   $\mu\text{m/s}$  and different temperature gradients

$G=30$  K/mm, the tensile strength is improved from 69 MPa at growth rate of 10  $\mu\text{m/s}$  to 179 MPa at a growth rate of 200  $\mu\text{m/s}$ , the elongation decreases from 20% at a growth rate of 10  $\mu\text{m/s}$  to 4% at a growth rate of 200  $\mu\text{m/s}$ . At  $v=200$   $\mu\text{m/s}$ , the tensile strength is improved from 94 MPa at a temperature gradient of 20 K/mm to 151 MPa at the temperature gradient of 30 K/mm, the elongation decreases from 18% at a temperature gradient of 20 K/mm to 11% at a temperature gradient of 30 K/mm. It is very clear that the growth rate and temperature gradient have significant effects on the room temperature mechanical properties of the Mg–2.35Gd alloy.

The improved tensile strength can be attributed to the finer microstructure and the smaller size of the intergranular phase with increasing growth rate and temperature gradient (cooling rate). It is known that, the tensile strength of the cellular structure is dependent on the cellular arm spacing. As shown in Figs. 2 and 4, the cellular spacing  $\lambda$  is indeed smaller with increasing growth rate and temperature gradient. And the strength of the experimental Mg–2.35Gd alloy would be improved. However, further investigation on the reduced elongation is still required.

## 4 Conclusions

1) The microstructure of the directionally solidified Mg–2.35Gd alloy exhibits a typical cellular structure and the cellular spacing  $\lambda$  decreases with increasing growth rate  $v$  for constant temperature gradient  $G$  and with increasing  $G$  for constant  $v$ . By a linear regression analysis, the relationships can be expressed as  $\lambda=136.216v^{-0.244}$  ( $G=30$  K/mm) and  $\lambda=626.5630G^{-0.5625}$  ( $v=10$   $\mu\text{m/s}$ ).

2) The values of the cellular spacing calculated by Kurz–Fisher model and Hunt model obviously diverge from the measured results, while the measured results are in a good agreement with the values calculated by Trivedi model. The Trivedi model could be used to predict the cellular spacing of Mg–2.35Gd alloy at  $G$  values of 20–30 K/mm and  $v$  values of 10–200  $\mu\text{m/s}$  with a reasonable accuracy.

3) The directionally solidified Mg–2.35Gd alloy exhibits improved strength than the non-directionally solidified alloy. The tensile strength of the directionally solidified experimental alloy is improved with increasing growth rate and/or temperature gradient.

## References

- [1] GÜNDÜZ M, CADIRLI E. Directional solidification of aluminium–copper alloys [J]. *Materials Science and Engineering A*, 2002, 327(2): 167–185.

- [2] FU Heng-zhi, GUO JING-jie, LIU Lin. Directional solidification and processing of advanced materials [M]. Beijing: Science Press, 2008: 237–251. (in Chinese)
- [3] ZHANG C, MA D, WU K S, CAO H B, CAO G P, KOU S. Microstructure and microsegregation in directionally solidified Mg–4Al alloy [J]. Intermetallics, 2007, 15(10): 1395–1400.
- [4] ZHENG X W, LUO A L, ZHANG C, DONG J, WALDO-RICHARD A. Directional solidification and microsegregation in a magnesium–aluminum–calcium alloy [J]. Metall and Mat Trans A, 2012, 43(9): 3239–3248.
- [5] PETERSEN K, LOHNE O, RYUM N. Dendritic solidification of magnesium alloy AZ91 [J]. Metall Mater Trans A, 1990, 21(1): 221–230.
- [6] MIRKOVIĆ D, SCHMID-FETZER R. Directional solidification of Mg–Al alloys and microsegregation study of Mg alloys AZ31 and AM50: Part II. Comparison between AZ31 and AM50 [J]. Metall Mater Trans A, 2009, 40(4): 974–981.
- [7] GAO Lei, CHEN Rong-shi, HAN En-hou. Effects of rare-earth elements Gd and Y on the solid solution strengthening of Mg alloys [J]. Journal of Alloys and Compounds, 2009, 481(1–2): 379–384.
- [8] WANG Jun, MENG Jian, ZHANG De-ping, TANG Ding-xiang. Effect of Y for enhanced age hardening response and mechanical properties of Mg–Gd–Y–Zr alloys [J]. Materials Science and Engineering A, 2007, 456(1–2): 78–84.
- [9] NISHIJIMA M, HIRAGA K. Structural changes of precipitates in an Mg–5at%Gd alloy studied by transmission electron microscopy [J]. Materials Transactions, 2007, 48(1): 10–15.
- [10] HONMA T, OHKUBO T, KAMADO S, HONMA K. Effect of Zn additions on the age-hardening of Mg–2.0Gd–1.2Y–0.2Zr alloys [J]. Acta Materialia, 2007, 55(12): 4137–4150.
- [11] NIE Jian-feng, GAO Xiang, ZHU Su-ming. Enhanced age hardening response and creep resistance of Mg–Gd alloys containing Zn [J]. Scripta Materialia, 2005, 53(9): 1049–1053.
- [12] LIU Shao-jun, YANG Guang-yu, JIE Wan-qi. A crucible and its preparation methods for magnesium alloys directional solidification: China, 201210014615.5 [P]. 2013–05–01. (in Chinese)
- [13] KURZ W, FISHER D J. Dendrite growth at the limit of stability: Tip radius and spacing [J]. Acta Materialia, 1981, 29(1): 11–20.
- [14] KURZ W, FISHER D J. Fundamentals of solidification [M]. London: Trans Tech Publications, 1998: 11–30.
- [15] LU S Z, HUNT J. A numerical analysis of dendritic and cellular array growth: The spacing adjustment mechanisms [J]. Journal of Crystal Growth, 1992, 123(1): 17–34.
- [16] HUNT J, LU S Z. Numerical modelling of cellular and dendritic array growth: Spacing and structure predictions [J]. Materials Science and Engineering A, 1993, 173(1): 79–83.
- [17] HUNT J, LU S Z. Numerical modeling of cellular/dendritic array growth: Spacing and structure predictions [J]. Metall Mater Trans A, 1996, 27(3): 611–623.
- [18] TRIVEDI R. Interdendritic spacing: Part II. A comparison of theory and experiment [J]. Metall Mater Trans A, 1984, 15(6): 977–982.

## Mg–2.35Gd 合金的定向凝固 显微组织与室温力学性能

王甲贺<sup>1,2</sup>, 杨光昱<sup>1,2</sup>, 刘少军<sup>1,2</sup>, 介万奇<sup>1,2</sup>

1. 西北工业大学 材料学院, 西安 710072;
2. 西北工业大学 凝固技术国家重点实验室, 西安 710072

**摘要:** 研究定向凝固条件下凝固参数(生长速率  $v$  和温度梯度  $G$ )对 Mg–2.35Gd 合金显微组织及室温力学性能的影响。采用金属液淬技术, 在温度梯度  $G$  为 20、25、30 K/mm, 生长速率  $v$  为 10–200  $\mu\text{m/s}$  条件下通过高梯度 Bridgman 定向凝固炉制备试样。研究表明, 实验合金的显微组织均为胞晶组织, 胞晶间距  $\lambda$  随温度梯度和生长速率的增大而减小, 其非线性拟合关系分别为  $\lambda=136.216v^{-0.2440}$  ( $G=30$  K/mm)、 $\lambda=626.5630G^{-0.5625}$  ( $v=10$   $\mu\text{m/s}$ ), 均与 Trivedi 模型较吻合。随温度梯度和生长速率的增大, 合金室温抗拉强度逐渐提高, 伸长率逐渐降低。同时, 合金室温抗拉强度高于相同冷却速率条件下自由凝固试样的室温抗拉强度。

**关键词:** Mg–2.35Gd 合金; 定向凝固; 胞晶间距; 显微组织; 力学性能

(Edited by Wei-ping CHEN)